CANCER GENOMICS & PROTEOMICS *22*: 326-345 (2025)
doi: 10.21873/cgp.20504

DEFA1, Primarily Expressed at the Invasive Tumor Front, Promotes OSCC Cell Invasion and Tumor Growth

HOJIN JEONG[1*], SANG WOONG PARK[2*] and YOUNG SUN HWANG[1*]

[1]Department of Dental Hygiene, College of Health Science, Eulji University, Seongnam, Republic of Korea;
[2]Department of Paramedicine, College of Health Science, Eulji University, Seongnam, Republic of Korea

Abstract

Background/Aim: The tumor microenvironment greatly influences cancer occurrence, progression, and treatment resistance, making it a key target alongside cancer cells. In squamous cell carcinoma, the invasive front is crucial for studying invasion mechanisms driven by the surrounding microenvironment and for identifying biomarkers to diagnose and predict invasive cancer. In this study, we aimed to elucidate the regulation of cancer characteristics through the interactions between factors at the invasive tumor front and the surrounding tumor microenvironment.
Materials and Methods: The invasive tumor front (ITF) and tumor center (TC) of collective cancer invasion were analyzed using microarray to compare gene expression. A stable cell line with depleted DEFA1 expression was established, and its effect on cancer growth was observed using a mouse tongue xenograft model. Invasive activity was assessed using Transwell assays. Gene profiling of cancer cells and analysis of secreted proteins interacting with U937 monocytic cells during co-culture were conducted using QuantSeq 3' mRNA sequencing and LC-MS/MS analysis.
Results: DEFA1 was overexpressed at the ITF of collective cancer invasion. YD10B cells with depleted DEFA1 expression exhibited significantly reduced invasiveness and tumor growth without changes in the cell cycle distribution. Co-culture with U937 cells significantly enhanced the invasiveness of YD10B cells, which was inhibited by anti-DEFA1 treatment. QuantSeq 3' mRNA sequencing and LC-MS/MS analyses confirmed that DEFA1 derived from U937 cells increased the invasiveness of YD10B cells. Recombinant DEFA1 (rDEFA1) significantly enhanced the invasiveness of YD10B cells *via* the JNK MAPK/NF-κB signaling pathway, independent of changes in DEFA1 expression within YD10B cells.
Conclusion: DEFA1 is crucial for cancer invasion and growth, and monocyte-derived DEFA1 exacerbates these traits. This study highlights DEFA1's role in promoting invasion at the tumor front, where interactions with the microenvironment are active.

Keywords: Defensin-1 alpha, collective cancer invasion, invasive tumor front, tumor microenvironment, monocyte.

*These Authors contributed equally to this work.

Professor Young Sun Hwang, Department of Dental Hygiene, College of Health Science, Eulji University, Sanseong-Daero 553, Sujeong-Gu, Seongnam, 13135, Republic of Korea. E-mail: kiteys@eulji.ac.kr

Received November 8, 2024 | Revised December 5, 2024 | Accepted December 16, 2024

Introduction

In many types of human malignant epithelial tumors, cancer cells exhibit collective invasion into the surrounding stroma instead of disseminating individually. Collective cancer invasion involves coordinated movement of groups of connected cancer cells, facilitating tumor progression and potential metastasis (1). This coordinated migration involves cancer cell populations collectively invading surrounding tissues. Such collective behavior is common during the development of tissues and organs in embryonic and perinatal stages. However, in the adult body, with the exception of certain white blood cells, immune cells, and mesenchymal stem cells, most somatic cells migrate locally to reorganize or remodel tissue structures without movement (2). Cell migration involves remodeling and reorganization of the cytoskeleton, including actin filaments, microtubules, and intermediate filaments, which are tightly regulated by various signaling pathways and chemical induction signals from soluble growth factors, chemokines, and cytokines (3). Mechanisms that regulate physical forces of attachment to the extracellular matrix (ECM), gene expression regulation, and cell polarity and membrane transport are also crucial for cell migration. The collective cancer invasion mechanism is characterized by plasticity in cell-cell interactions, integrin function, and migration strategies that contribute to the dynamic movement of cancer cells (4-6). Collective cancer invasion is driven by heterogeneous groups of tumor cells polarized into a 'leading edge' or 'invasion front' (7). The characteristics of the invasive tumor front of a collective cancer differ significantly from those of the tumor center (8). The tumor center in collective cancer invasions often exhibits high expression of E-cadherin (1). E-cadherin-mediated cell adhesion promotes collective cell migration, where cell populations move coherently while maintaining intercellular connections. Accumulating studies have identified molecules specifically expressed at the invasive tumor front of collective cancer invasion, such as podoplanin (9), insulin-like growth factor 2 mRNA-binding protein 3 (10), basal epithelial genes (11), Rac, integrin β1, and PI3K proteins (12), RAB13 and NET1 RNAs (13), NF-kB-inducing kinase (NIK) gene (14), and DNA methylation and gene expression variations (15). These proteins collectively contribute to the unique properties of collective cancer invasion, supporting coordinated movement, cell-cell interactions, and invasion at the invasive tumor front.

The tumor microenvironment (TME) is composed of fibroblasts, immune cells, bone marrow-derived inflammatory cells, signaling molecules, and extracellular matrix (ECM) (16). In the TME, cancer cells can promote new blood vessels and induce peripheral immune tolerance, which can significantly impact cancer development, progression, metastasis, and treatment resistance. Cancer-associated fibroblasts (CAFs), tumor-associated macrophages (TAMs), and other immune and inflammatory cells in the TME originally can inhibit cancer cell growth. However, they eventually support cancer activity in early stages of cancer progression. These components can suppress immune cells and create a favorable environment for cancer growth or metastasis. Consequently, targeted treatments addressing both cancer cells and the TME have been proposed to prevent cancer recurrence and metastasis and to enhance the effectiveness of drug and radiation therapies. Collective invasion of cancer cells is influenced by various cells and the extracellular matrix within the TME (17). Cancer invasion is maintained through the activation of signaling pathways that can regulate cytoskeleton dynamics such as invadopodia through actin polymerization by regulatory proteins like cortactin and N-WASP (18). Invadopodia can focally secrete protease enzymes, mainly matrix metalloproteases (MMPs), to degrade the ECM and create pathways for cancer cell invasion. The invasion front is the interface between the tumor and host tissue. It is a critical region for progression and metastasis of malignant cells. Invadopodia formation is highly active in the invasion front. Therefore, studies have focused on genes specifically expressed at the invasive tumor front and the influence of regional cancer microenvironment (19-22). However, the exact mechanisms and key factors of cancer invasion and subsequent metastasis are not fully understood yet.

Various isoforms of defensing-alpha (DEFA) have been reported in lung, skin, and urogenital epithelial cells, with DEFA6 found to be elevated in sera samples of patients with colorectal cancer, suggesting its potential as a diagnostic marker for colorectal cancer (23). DEFA1 is a cationic amphipathic peptide with broad-spectrum antimicrobial properties. It is known for its role in host defense, including antimicrobial immunity and cytotoxicity (24). We performed gene expression profiling of invasive tumor front and tumor center areas in tissues with collective cancer invasion and confirmed that the expression of defensin-1 alpha (DEFA1) was increased specifically at the invasive tumor front. However, the role and regulation of DEFA1 in cancer cells and the tumor microenvironment have not been precisely identified yet. Thus, this study aimed to elucidate the role of DEFA1 found to be overexpressed at the invasive tumor front by establishing a *DEFA1* knockdown cell line to assess its impact on invasion activity and tumor growth. Additionally, this study investigated the regulation of DEFA1 expression by the tumor microenvironment using co-culture techniques, with the goal of elucidating intricate interactions between the invasive tumor front and the surrounding tumor microenvironment.

Materials and Methods

Cell culture. The human YD10B oral squamous cell carcinoma cell line was cultured in DMEM/F12 (3:1 ratio) medium (Gibco BRL Co., Rockville, MD, USA) supplemented with 10% fetal bovine serum, 1×10^{-10} M cholera toxin, 0.4 mg/ml hydrocortisone, 5 μg/ml insulin, 5 μg/ml apo-transferrin, and 2×10^{-11} M triiodothyronine (T3) (21). The human acute monocytic leukemia cell line U937 was cultured in RPMI1640 media (Gibco) supplemented with 10% FBS, 1% penicillin/streptomycin, and 50 μg/ml neomycin in a humidified 5% CO_2 incubator (Thermo Fisher Scientific, Waltham, MA, USA). The cell lines were purchased from the Korean Cell Line Bank (Seoul, Republic of Korea), and their genetic identity was confirmed through DNA fingerprinting analysis using short tandem repeat (STR) markers. U937 cells were differentiated into macrophages with 100 nM phorbol 12-myristate 13-acetate (PMA) prior to co-culture. After 48 h, only the cells attached to the bottom of the culture flask were harvested for analysis.

Microarray analysis. Frozen surgical tissues from patients diagnosed with OSCC were analyzed in areas with a collective cancer invasion (n=3). From October to December 2022, portions of excised tissue were collected from patients diagnosed with OSCC who underwent surgical procedures at Eulji University Hospital (Daejeon, Republic of Korea). The age, sex, biopsy site, differentiation, and TNM stage of the patients who consented to the use of their tissues are as follows: Patient 1 (63 years old, female, tongue, well to moderately differentiated, T2N0M0), Patient 2 (70 years old, male, tongue, moderately differentiated, T2N1M0), Patient 3 (61 years old, male, tongue, moderately differentiated, T2N0M0). From frozen-sectioned surgical tissues, the invasive tumor front (ITF) and tumor center (TC) of the collective invasion were separated and harvested under a digital microscope (EVOS XL Core Imaging System, Thermo Fisher Scientific, Bothell, WA, USA) using a fine spatula blade (Thomas Scientific, Swedesboro, NJ, USA). RNA was extracted and gene expression was compared using the Human Gene ST 2.0 analysis (Affymetrix Inc., Santa Clara, CA, USA). Microarray analysis data were obtained using an Affymetrix 3000 7G scanner. The gene values extracted through microarray analysis were calculated as the ratio of the signal value of TC to the signal value of ITF. The sample adequacy and microarray analysis of the extracted RNA were performed using a BioCore instrument (BioCore Co., Ltd., Seoul, Republic of Korea). For the use of human specimens, informed consent was obtained from the patients, and approval was received from Eulji University's Institutional Review Board (Sep 14, 2022) (IRB number; EU22-57), and the study was conducted in accordance with the Declaration of Helsinki. All patients provided written informed consent to participate in the study.

Construction of a stable cell line with suppressed DEFA1 expression. For construction of a stable cell line with suppressed *DEFA1* expression, a *DEFA1* shRNA expression vector in a pGFP-C-shLenti plasmid (TL320804) (OriGene, Rockville, MD, USA) was used to generate *DEFA1* knockdown YD10B cells. The Lenti-vpak Lentiviral Packaging kit, containing four unique 29-mer shRNA constructs in a lentiviral GFP vector (TL320804A-D) and a scrambled negative control non-effective shRNA cassette (TR30021), was utilized. The shRNA sequences are as follows: (TR30021; gcactaccagagctaactcagatagtact, TL320804A; aacgtcgctatggaacctgcatctaccag, TL320804B; gtgcattgcagga gaacgtcgctatggaa, TL320804C; catctacca gggaagactct gggcattct, TL320804D; ccatccttgctgccattc tcctggtggcc). Lentivirus particles were produced in 293FT cells (Invitrogen, Carlsbad, CA, USA), purified using a 0.22 μm filter, and titrated. To establish *DEFA1* knockdown stable cancer cell lines, YD10B cells were transduced with 1×10^7 lentiviral particles in the presence of the transduction enhancer Polybrene (10 μg/ml, Sigma-Aldrich). Lentiviral particles produced with the scrambled negative control shRNA cassette were used to establish a wild-type stable cell line (siCon-WT). After 24 h of viral introduction, puromycin (10 μg/ml) (Gibco, Grand Island, NY, USA) was added to the medium to select puromycin-resistant cells. The degree of *DEFA1* knockdown was confirmed by western blot analysis. All gene silencing procedures were conducted according to the manufacturer's instructions.

Mouse tongue xenograft. All animal procedures were performed in accordance with the Guide for the Care and Use of Laboratory Animals published by the US National Institutes of Health, and all animal experiments were approved by the Institutional Animal Care and Use Committee of Eulji University (EUIACUC22-13). Thirty-five male Balb/c *nu/nu* mice (4 weeks old; body weight, 11±2.5 g) were purchased from Jungang Animal Inc. (Seoul, Republic of Korea) and were maintained under a 12-h light/dark cycle at 20-22˚C SPF condition. The mice were allowed to acclimate for one week after arrival at the animal facility before use in the experiments. If a weight loss exceeding 20% occurred compared to the body weight of control mice that were not transplanted with cancer cells, the experiment was terminated prior to reaching the planned endpoint. Anesthesia was induced using Zoletil (30 mg/kg; Verbac, Carros, France) *via* intraperitoneal injection, and the stability of anesthesia was monitored by assessing the heart rate. Cells (5×10^4 cells/0.1 ml in media) were injected intramuscularly into mouse tongues under anesthesia, and the mice were observed for 6 weeks with regular monitoring of body weight and diet. Following cancer cell transplantation, the mice were monitored with the provision of fresh food and water every three days, and no individuals were prematurely excluded from the experiment due to weight loss. At the conclusion of the experiments, the mice were sacrificed by cervical dislocation, and the cessation of heartbeat was monitored for 2 to 3 minutes to confirm death. Tumor volume was calculated using the formula: volume = (length × width^2)/2. To confirm tumor growth, the tongues were harvested, fixed in paraformaldehyde, and analyzed pathologically.

Immunohistochemistry and H&E staining. For immuno-staining, tissue sections were deparaffinized using xylene for antigen retrieval and subsequently blocked with 5% normal goat serum for 3 h. The tissue sections were then incubated with a DEFA1 primary antibody (NBP3-05562, Novus Biologicals, Centennial CO, USA) at a 1:100 dilution for 1 h, followed by three rinses with PBS. Next, the sections were incubated with biotinylated anti-mouse/anti-rabbit IgG (H + L) (BA-100-2.2, Vector Laboratories, Inc., Newark, CA, USA) at a 1:200 dilution for 30 minutes and rinsed three times with PBS. This was followed by a reaction with horseradish peroxidase-conjugated streptavidin (SA-5704-100, Vector Laboratories, Inc.) at a 1:300 dilution for 30 minutes, after which the cells were rinsed three times with PBS. The tissue sections were then stained with 3,3'-diaminobenzidine (DAB) and counterstained with hematoxylin before being observed under a microscope (EVOS XL Core Imaging System). All procedures were performed at room temperature. For histological

analysis, sections were deparaffinized with xylene and stained with hematoxylin and eosin.

Transwell invasion assay. Polycarbonate nucleopore Transwell inserts with 8 μm pores (Corning Inc., NY, USA) were coated with collagen (30 μg/well; Becton Dickinson, Lincoln Park, NJ, USA) for 1 h. Cells (5×10^4 cells/insert) were added to the collagen-coated inserts, and 0.9 ml of complete media was added to the lower chamber for incubation 37˚C. After 48 h, the filter inserts were removed, and the cells attached to the lower chamber were imaged and counted using the EVOS XL Cell Imaging System (Thermo Fisher Scientific, Waltham, MA, USA). To measure the effects of recombinant DEFA1 (rDEFA1), rDEFA1 (2 and 10 μg/ml) (PHC1615, GIBCO, Waltham, MA, USA) was added to the media in the lower chamber.

Western blot analysis. For the Western blot analysis, cells were lysed using RIPA buffer (Sigma) containing protease inhibitor cocktail tablets (Merck KGaA, Darmstadt, Germany), and the supernatant obtained after centrifugation was used for analysis. Proteins were quantified using the Bradford assay, and equal amounts of protein (50 μg) were separated on a 15% SDS-PAGE gel. The proteins were then transferred to a polyvinylidene difluoride (PVDF) membrane (Millipore, Billerica, MA, USA) and blocked with 5% skim milk at room temperature. The membrane was sequentially incubated with the primary antibody (1:1,000 dilution) and HRP-conjugated secondary antibody (1:3,000 dilution, anti-rabbit; #7074, anti-mouse; #7076) (Cell Signaling Technology, Danvers, MA, USA). The target proteins were detected using an Enhanced Chemiluminescence (ECL) Detection kit (Amersham Life Science, Parsippany, NJ, USA). The antibodies used for the analysis are as follows: Anti-SAPK/JNK (#9252), phospho-SAPK/JNK (Thr183/Tyr185) (#4668), Anti-p44/42 (Erk1/2) (#4695), phospho-p44/42 (Erk1/2) (Thr202/Tyr204) (#4370), Anti-p38 MAPK (#9212), phospho-p38 MAPK (Thr180/Tyr182) (#4511), Anti-Akt (#9272), phospho-Akt (Ser473) (#4060), and Lamin A/C (#4777), all obtained from Cell Signaling. Anti-DEFA1 (NBP3-05562) and anti-β-actin (AC-15) were acquired from Novus Biologicals (Centennial, CO, USA). Protein levels were compared by calculating the relative signal intensity of the pixel area of the region of interest using ImageJ software ver 1.53i (National Institutes of Health).

Cell cycle distribution. To analyze the cell cycle of the stable cell line, FACS analysis was performed. Cells cultured in a 100 mm dish to 70% confluence were harvested by trypsinization and then fixed with cold ethanol for 2 h. The cells were sequentially treated with 0.25 μg/ml of RNase A (Sigma) and 50 μg/ml of propidium iodide (PI, Invitrogen). The DNA content for cell cycle distribution was analyzed using a FACSCalibur apparatus with WinMDI 2.9 software (BD Biosciences, Franklin Lakes, NJ, USA).

Enzyme-linked immunosorbent assay (ELISA). The DEFA1 level was quantified using the Human Alpha-Defensin 1 DuoSet ELISA kit (R&D Systems) (DY8198-05) (R&D Systems, Minneapolis, MN, USA) according to the manufacturer's protocols. Cells cultured in a 12-well culture dish were washed twice with PBS and then incubated in serum-free medium (1 ml) for 24 h at 37˚C. The supernatant from the culture medium was collected after centrifugation at 1,000 × *g* for 10 min and used as the analytical sample. The absorbance was measured with a microplate reader.

Calcein-AM labeling and co-culture. The cancer cells (5×10^4 cells) were suspended in 1 ml of serum-free media, and Calcein-AM (final concentration of 50 μM, C1430, Invitrogen, Waltham, MA, USA) was added. The cells were then incubated for 30 minutes at room temperature in the dark. After incubation, the cells were centrifuged, collected, and added to collagen-coated Transwell inserts. U937 cells (5×10^4 cells) were added to the lower chamber without Calcein-AM labeling. To observe the effect of the DEFA1 antibody, the antibody (2 μg/ml, NBP3-05562) was added to both the Transwell inserts and the lower chamber. The cells were incubated

for 24 h in serum-free media at 37˚C, after which the cells attached to the lower chamber were harvested using 0.25% Trypsin-EDTA and subjected to fluorescence analysis (Excitation ~488 nm/Emission ~517 nm) using a microplate reader (Synergy™ HTX Multi-Mode Microplate Reader; BioTek Instruments Inc., Winooski, VT, USA).

Co-culture of YD10B and U937 cells. To observe signaling molecules and intracellular gene expression changes involved in the interaction between the two cell types, YD10B and U937 were co-cultured. Transwell-COL permeable supports (collagen-coated, 24 mm insert; Costar Corning Inc., Kennebunk, ME, USA) with a 0.4 μm membrane pore size impermeable to cells were used for this purpose. YD10B cells (1×10^6) were added to the Transwell supports, and U937 cells (1×10^6) were added to the lower chamber. The cells were co-cultured in media containing 1% FBS for 48 h at 37˚C. Cells were harvested from the Transwell supports for Western blot analysis and gene expression profiling. The culture medium was collected for LC-MS/MS analysis.

QuantSeq 3' mRNA-Sequencing for gene expression profiling. Total RNA was isolated from cultured cells using Trizol reagent (Invitrogen). The quality of the extracted RNA was evaluated using the Agilent TapeStation system (Agilent Technologies, Amstelveen, the Netherlands), while RNA concentration was measured *via* the Qubit assay (Thermo Fisher Scientific). To prepare libraries, the QuantSeq 3' mRNA-Seq Library Prep Kit (Lexogen, Vienna, Austria) was employed, following the provided protocol. The processes of library amplification for adapter sequence introduction, sequencing, QuantSeq 3' mRNA-Seq data analysis, and gene expression quantification using HTSeq-count were conducted in accordance with established protocols described in previous studies (25, 26). A heatmap generated through hierarchical clustering was processed and examined using ExDEGA GraphicPlus. Data mining and graphic visualization were performed using ExDEGA (Ebiogen Inc., Seoul, Republic of Korea).

LC-MS/MS analysis. Proteins extracted from GCF samples (25 μg) by precipitation with acetone were dissolved in 5% SDS buffer (5% SDS, 50 mM TEAB, pH 7.55). Solubilized proteins were digested using S-Trap™ micro spin columns (Protifi, Farmingdale, NY, USA) according to the manufacturer's instructions. For mass spectrometry, protein digests were eluted using trypsin/Lys-C protease, and fractionated peptides were obtained from a reversed-phase fractionation spin column (Thermo Fisher Scientific, Rockford, IL, USA) using a serial percent solution of acetonitrile. Peptide samples were separated sequentially using a Q Exactive™ HF-X hybrid quadrupole-orbitrap mass spectrometer (Thermo Fisher Scientific) and a trap column (100 mm × 2 cm) filled with Acclaim PepMap100 C18 resin. Tandem mass spectra were acquired with an Orbitrap mass analyzer using a mass resolution of 15,000 at m/z 200. Protein identification and quantification of LC-MS/MS raw data files were performed with Proteome Discoverer 2.4 software (Thermo Fisher Scientific). All analysis procedures were conducted according to the manufacturer's instructions (27).

Statistical analysis. All statistical analyses were conducted using the InStat GraphPad Prism ver. 5.01 software (GraphPad Software, Inc., San Diego, CA, USA). The significance of the expression differences between the tumor center and invasive tumor front was evaluated using the Mann-Whitney *U*-test. The significance of tumor volume, invasion activity, DEFA1 concentration, and band intensity in the western blot analysis were assessed using the Kruskal-Wallis test with Dunn's multiple comparison testing. *p*-Values of less than 0.05 were considered statistically significant.

Ethics approval statement and consent to participate. For the use of human specimens, approval was received from Eulji University's Institutional Review Board (IRB number; EU22-57), and the study was conducted in accordance with the Declaration of Helsinki. All patients provided written informed consent to participate in the study. Animal study

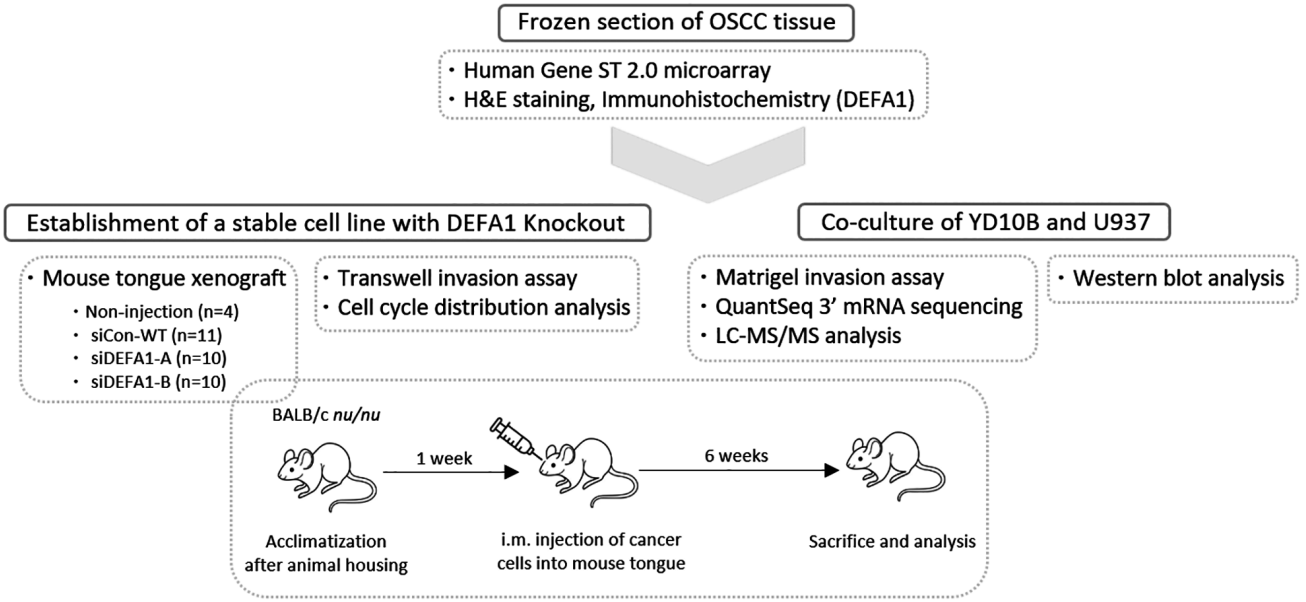

Figure 1. *The overall workflow of this study.*

was approved by the Institutional Animal Ethics Committee of Eulji University (EUIACUC22-13) and performed according to the Guide for the Care and Use of Laboratory Animals (NIH Publication no. 85-23, revised 1996).

Results

DEFA1 is overexpressed at the invasive tumor front in collective cancer invasion. The overall workflow of this study is presented in Figure 1. We easily observed collective cancer invasion on HE-stained slides of tissues from an oral cancer patient diagnosed with squamous cell carcinoma (Figure 2A). From frozen surgical tissues of patients diagnosed with OSCC, the collective cancer invasion area was divided into the highly invasive tumor front (ITF) and the tumor center (TC). Tissues were separated, and microarray analysis was performed to profile genes with more than a two-fold difference in expression. As a result, a significant difference (p=0.038) in expression was found for defensin-alpha 1 (*DEFA1*, gene accession; ENST00 000382679) belonging to the alpha defensin family (Table I). The average signal intensity of *DEFA1* was 94.924 in ITF and 27.514 in TC, indicating a 3.45 times higher signal in ITF. No significant expression changes were observed for genes of the beta defensin family. The expression of DEFA1 was confirmed by immunostaining compared to an antibody isotype control (IgG2a) in the collective cancer invasion area of squamous cell carcinoma, showing a particularly strong staining in ITF (Figure 2B).

Role of DEFA1 in cancer invasion and tumor growth. To elucidate the role of DEFA1 in cancer progression, we established YD10B OSCC cell lines in which *DEFA1* expression was suppressed using shRNA (Figure 3A). Among these, YD10B shRNA-A (siDEFA1-A) and shRNA-B (siDEFA1-B) cell lines with DEFA1 protein expression effectively suppressed were used to perform xenografts on mouse tongues to confirm the role of DEFA1 in tumor growth. As shown in Figure 3B, tumor volumes of tongues injected with the wild type (siCon-WT) were significantly larger than those of the negative control (non-injection) (519±51.8 *vs.* 132.5±25.9, p<0.001). Conversely, tumor volumes of tongues injected with

Table I. *The gene expression of defensin isoforms in the invasive tumor front (ITF) and tumor core (TC) regions within a collective cancer invasion of oral squamous cell carcinoma (OSCC) tissue was analyzed using microarray analysis.*

Gene description	Gene symbol	Gene accession	Signal for tumor center (C) (N=3, mean)	Signal for invasive tumor front (M) (N=3, mean)	Fold change [M *vs.* C]	*p*-Value [M *vs.* C]
Defensin, alpha 1	*DEFA1*	ENST00000382679	27.514	94.924	3.449	**0.038**
Defensin, beta 123	*DEFB123*	ENST00000376309	28.899	57.285	1.982	0.265
Defensin, beta 136	*DEFB136*	NM_001033018	10.734	15.838	1.475	0.288
Defensin, beta 131	*DEFB131*	NM_001040448	6.887	9.351	1.357	0.516
Defensin, beta 124	*DEFB124*	NM_001037500	19.686	26.653	1.353	0.086
Defensin, beta 126	*DEFB126*	ENST00000382398	37.866	48.111	1.270	0.418
Defensin, beta 113	*DEFB113*	NM_001037729	24.161	28.918	1.196	0.572
Defensin, beta 117	*DEFB117*	DQ012021	9.343	10.985	1.175	0.855
Defensin, beta 121	*DEFB121*	NM_001011878	4.747	5.423	1.142	0.131
Defensin, beta 134	*DEFB134*	ENST00000526438	9.437	10.380	1.099	0.230
Defensin, beta 130	*DEFB130*	NM_001037804	4.652	5.005	1.075	0.501
Defensin, alpha 4, Corticostatin	*DEFA4*	ENST00000297435	28.127	28.211	1.002	0.937
Defensin, beta 129	*DEFB129*	NM_080831	6.131	5.485	0.894	0.191
Defensin, alpha 6, Paneth cell-specific	*DEFA6*	NM_001926	8.604	6.758	0.785	**0.032**
Defensin, alpha 5, Paneth cell-specific	*DEFA5*	NM_021010	15.363	11.452	0.745	0.055
Defensin, beta 1	*DEFB1*	ENST00000297439	17.598	12.700	0.721	0.434
Defensin, beta 4B // defensin, beta 4A	*DEFB4B// DEFB4A*	ENST00000318157// ENST00000318157	143.011	91.410	0.639	0.788

Statistically significant *p*-values are shown in bold.

siDEFA1-A (162±45.8), or siDEFA1-B (154.5±41.8) were significantly smaller than those of siCon-WT ($p<0.001$). Differences in tumor growth among siCon-WT, siDEFA1-A, and siDEFA1-B were further confirmed through HE staining of xenografted tissue sections (Figure 3C). In the siCon-WT tongues, several large tumor masses were observed (diameter of tumor: 3.170±0.183 mm - 1.936±0.117 mm). In contrast, in the siDEFA1-A and siDEFA1-B tongues, multiple tumor foci and numerous tumors of relatively smaller size were observed (siDEFA1-A: 0.524±0.275 mm – 0.113±0.037 mm, siDEFA1-B: 0.280±0.131 mm – 0.091±0.058 mm). To confirm the role of DEFA1 in cancer invasion, we observed invasion activity using a Matrigel-coated Transwell chamber. Compared to the number of invaded cells in siCon-WT (461.7±53.7) after 48 h, numbers of invaded cells in siDEFA1-A (105.3±15.3) and siDEFA1-B (110.8±20.33) were significantly lower (Figure 4A). FACS analysis was conducted to determine if the difference in the number of infiltrating cells between cell lines was due to different cell growth rates. Results showed no significant difference in cell cycles among groups (siCon-WT, siDEFA1-A, and siDEFA1-B) (P2; sub-G_1 phase, P3; G_0/G_1 phase, P4; G_2/M phase) (Figure 4B).

Role of DEFA1 in cancer cell invasion mediated by U937 monocytic cells. To investigate the role of DEFA1 in the enhancement of cancer cell invasion mediated by U937 monocytic cells, a co-culture experiment was conducted using Transwells coated with collagen type I (45 μg/well) as shown in Figure 5A. To distinguish between U937 cells and cancer cells, YD10B cells were labeled with Calcein-AM. Calcein-AM-labeled YD10B cells (siCon-WT or siDEFA1-A) were added to the upper chamber, while U937 cells without Calcein-AM labeling were added to the lower chamber and co-cultured for 24 h. After 24 h, all cells in the lower chamber were harvested and Calcein fluorescence was measured. Compared to the fluorescence level of the siCon-WT control cultured alone (9,531±1,730), the fluorescence level of siCon-WT

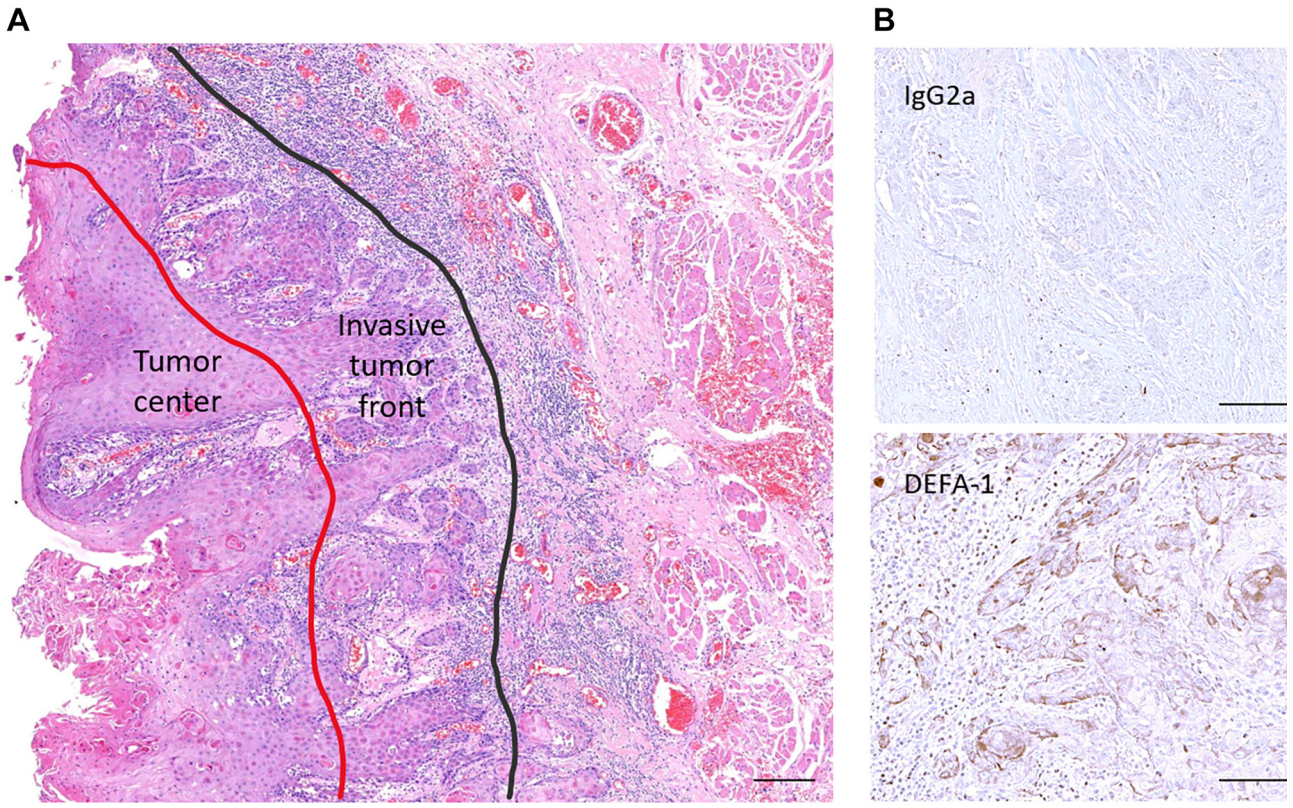

Figure 2. *Expression of DEFA1 in collective cancer invasion of oral squamous cell carcinoma (OSCC). (A) Hematoxylin and eosin (H&E) staining of squamous cell carcinoma tissue. The invasive tumor front (ITF) and tumor center (TC) regions were selected and delineated with solid lines in the collective cancer invasion for microarray analysis (magnification; 10×, scale bars: 100 μm). (B) Representative immunohistochemical analysis image showing DEFA1 expression in collective cancer invasion tissue. Hematoxylin was used for nuclear counterstaining. IgG2a served as an antibody isotype control (magnification; 20×, scale bars: 100 μm).*

co-cultured with U937 cells was significantly increased (30,794±4,433) ($p<0.001$) (Figure 5B). However, the increased fluorescence level of siCon-WT due to co-culture with U937 cells was significantly suppressed ($p<0.01$) to 14,130±3,257 after adding 2 μg/ml anti-DEFA1. In LC-MS/MS analysis, DEFA1 peptides were not detected in the conditioned media (CM) of siCon-WT, whereas two prominent DEFA1 peptides were detected in the CM of U937 cells (Accession P59665, neutrophil defensin 1) (Figure 5C). These two peptides (IPACIAGERR and YGTCIYQGR) were confirmed to match DEFA1 through alignment with a Reference Sequence (NP_004075.11) from NCBI (Figure 5D). Additionally, DEFA1 ELISA analysis showed no significant detection of DEFA1 in the CM of siCon-WT cells, whereas DEFA1 was detected in the CM of U937 cells at 286.5±20.14 ng/ml (Figure 5E). Moreover, the invasion of siCon-WT cells was increased by co-culturing these cells with U937 cells (27,844±4,264) or PMA-differentiated U937 cells (28,062±3,561) ($p<0.001$), showing no significant difference in the enhancement of cancer cell invasion between the two U937 cells (Figure 5F).

Regulation of DEFA1 expression and the invasion of cancer cells through co-culture with U937 monocytic cells. To investigate the expression of DEFA1 in cancer cells influenced by U937 monocytic cells, siCon-WT cells were co-cultured with U937 cells using Transwell-COL

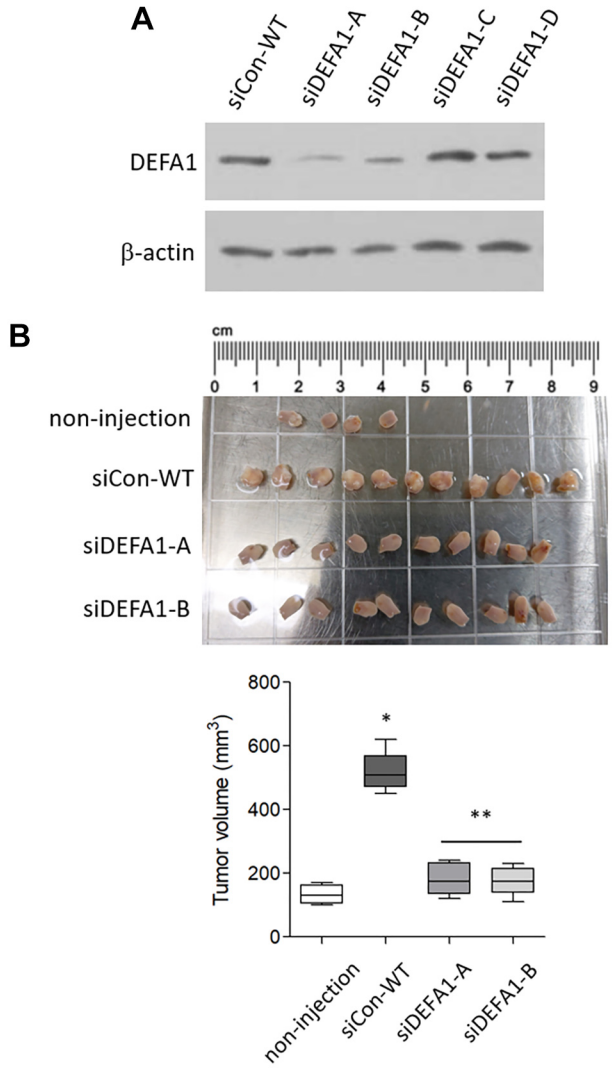

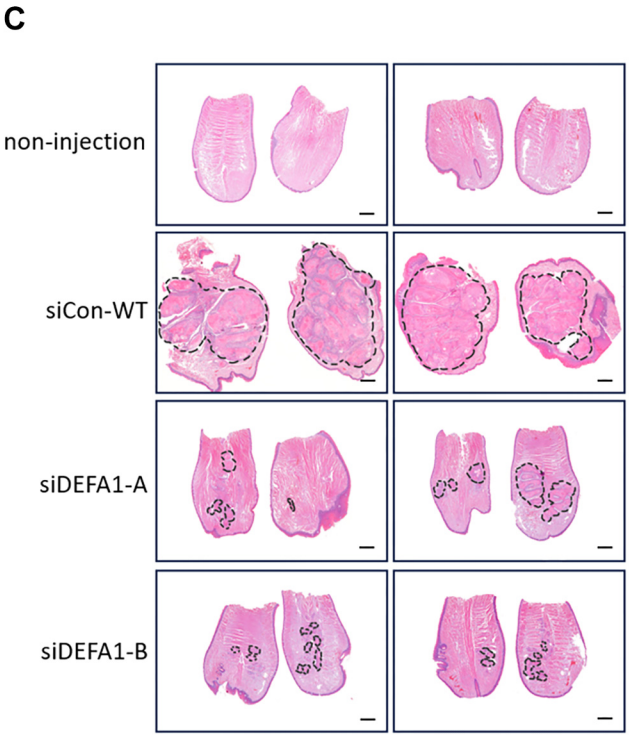

Group	Tongue tumor	
	Long diameter (mm, mean±SD)	Short diameter (mm, mean±SD)
non-injection (n=4)	-	-
siCon-WT (n=11)	3.170±0.183	1.936±0.117
siDEFA1-A (n=10)	0.524±0.275	multiple foci, 0.113±0.037
siDEFA1-B (n=10)	0.280±0.131	multiple foci, 0.091±0.058

Figure 3. *Role of DEFA1 in tumor growth. (A) Establishment of a stable YD10B oral squamous cell carcinoma (OSCC) cell line with DEFA1 knockdown using RNA interference. To create the DEFA1 knockdown cell line, lentiviral particles were introduced with four unique 29-mer shRNA constructs (siDEFA1-A, siDEFA1-B, siDEFA1-C, and siDEFA1-D) and a scrambled negative control ineffective shRNA cassette (siCon-WT). DEFA1 expression levels were analyzed by Western blot, with β-actin serving as a protein loading control. (B) Tumor growth analysis in a mouse tongue xenograft model with DEFA1 knockdown cell lines. Tumor volumes in the tongue were graphed for each group at six weeks after cell line introduction (non-injection; n=4, siCon-WT; n=11, siDEFA1-A; n=10, siDEFA1-B; n=10). *p<0.001 vs. non-injection, **p<0.001 vs. siCon-WT. (C) Representative H&E staining images of xenografted mouse tongues tissues (magnification; 4×, scale bars: 400 μm). The tumor locations are indicated with black dotted lines, and the long and short diameters of the tumors are provided in a table. mm: Millimeter, mean±SD: mean±standard deviation.*

permeable supports (0.4 μm pore, collagen-coated) for 24 h. Subsequently, siCon-WT cells from the Transwell were harvested and DEFA1 levels were analyzed *via* western blot. As shown in Figure 6A, DEFA1 levels in siCon-WT cells did not significantly change compared to their levels when co-cultured with U937 cells. Similarly, QuantSeq 3' mRNA-Sequencing of defensin family mRNA expression revealed that no difference in *DEFA1* level between siCon-WT cells

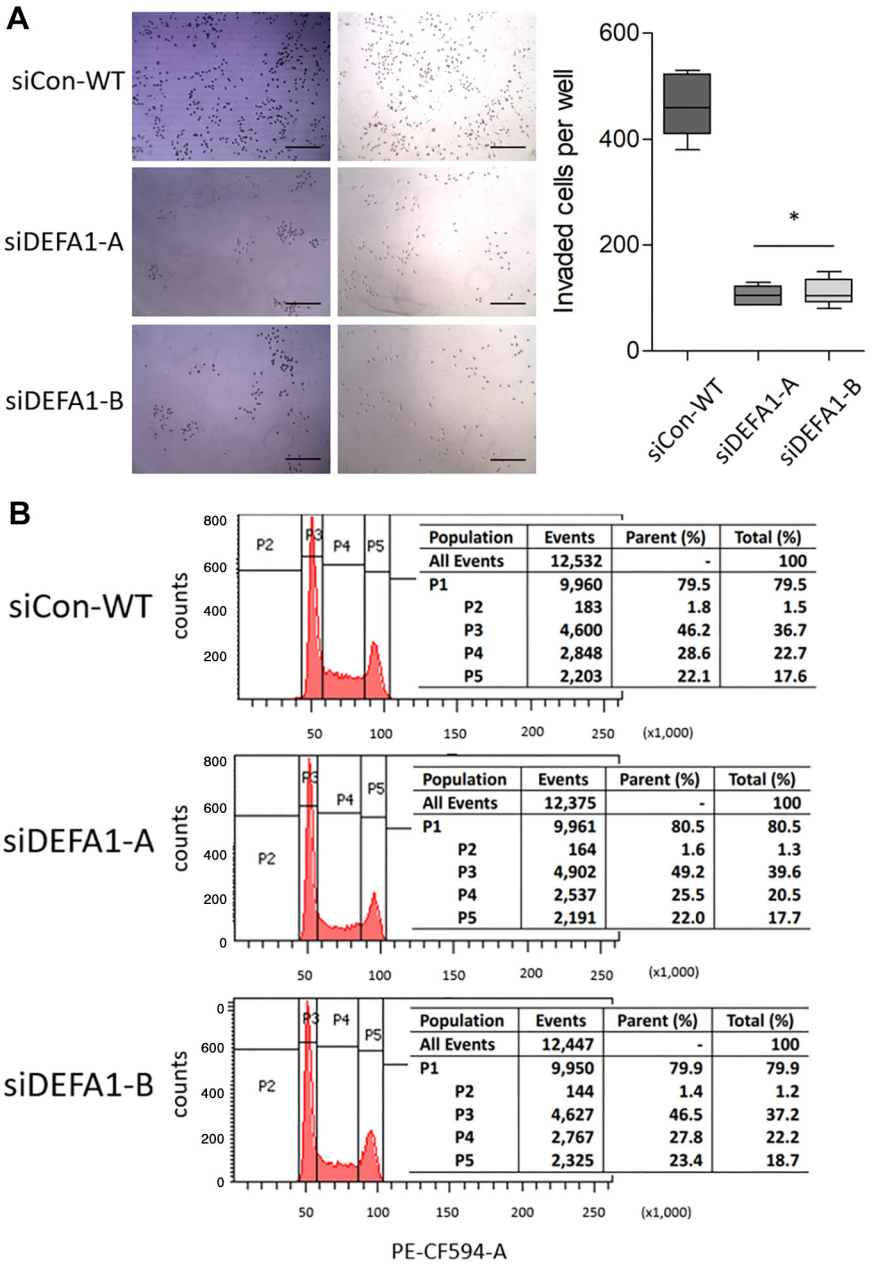

Population	Events	Parent (%)	Total (%)
All Events	12,532	-	100
P1	9,960	79.5	79.5
P2	183	1.8	1.5
P3	4,600	46.2	36.7
P4	2,848	28.6	22.7
P5	2,203	22.1	17.6

Population	Events	Parent (%)	Total (%)
All Events	12,375	-	100
P1	9,961	80.5	80.5
P2	164	1.6	1.3
P3	4,902	49.2	39.6
P4	2,537	25.5	20.5
P5	2,191	22.0	17.7

Population	Events	Parent (%)	Total (%)
All Events	12,447	-	100
P1	9,950	79.9	79.9
P2	144	1.4	1.2
P3	4,627	46.5	37.2
P4	2,767	27.8	22.2
P5	2,325	23.4	18.7

Figure 4. *Role of DEFA1 in cancer cell invasion. (A) An in vitro invasion assay was performed for 48 h using a Matrigel-coated Transwell. More than four repeated experiments were conducted. Two representative images are provided (magnification; 100×, scale bars: 200 μm). The number of cells that migrated to the lower chamber was counted and presented in a graph. *p<0.0001 vs. siCon-WT. (B) Flow cytometry analysis for cell cycle distribution. Equal numbers of cells were stained with propidium iodide. Cell cycle distributions are displayed as representative histograms. P2: Sub-G_1, P3: G_1, P4: S, P5: G_2/M.*

co-cultured with U937 cells and siCon-WT cells cultured alone (Figure 6B). This is illustrated in the hierarchical clustering heatmap [siCon-WT (co-culture with U937) *vs.* siCon-WT only *vs.* siCon-WT (co-culture with U937) *vs.* U937 only]. Instead of co-culturing with U937, recombinant DEFA1 (rDEFA1) was added to siCon-WT

cells and invasion was observed using collagen-coated Transwell chambers. After 24 h, the number of invading cells at the bottom of the chamber was counted. Compared to the number of invading siCon-WT cells cultured alone, the number of invading siCon-WT cells treated with 2 μg/ml or 10 μg/ml rDEFA1 was increased (Figure 6C). These results suggest that DEFA1 secreted from U937 cells can stimulate cancer invasion independently of any changes in DEFA1 levels within cancer cells.

Cell signal molecules in cancer cells influenced by co-culture with U937 monocytic cells. The signaling pathway related to cancer invasion in siCon-WT cells co-cultured with U937 was analyzed using western blotting (28). Compared to control cells not co-cultured with U937, the activation (phosphorylation) of c-Jun NH2-terminal kinase (JNK), a member of the mitogen-activated protein kinases (MAPKs), was significantly increased in siCon-WT cells co-cultured with U937 (Figure 7A). No significant changes were observed in the activation of extracellular signal-regulated kinases-1/2 (ERK1/2), p38 MAPK, and Akt. The enhanced activation of JNK induced by co-culture with U937 was markedly inhibited by treatment with 10 μg/ml rDEFA1. Additionally, we assessed the nuclear translocation levels of p50 and p65, components of the nuclear factor kappa-light-chain-enhancer of activated B cells (NF-κB) complex, which are critical in regulating cancer invasion and progression. To achieve this, cell extracts were fractionated into cytosolic and nuclear components for analysis. Compared to control cells, the levels of p50 and p65 in the nuclear fraction of siCon-WT cells co-cultured with U937 were increased (Figure 7B). The enhancement of nuclear translocation of p50 and p65 in cancer cells induced by co-culture with U937 was significantly reduced by treatment with 10 μg/ml rDEFA1.

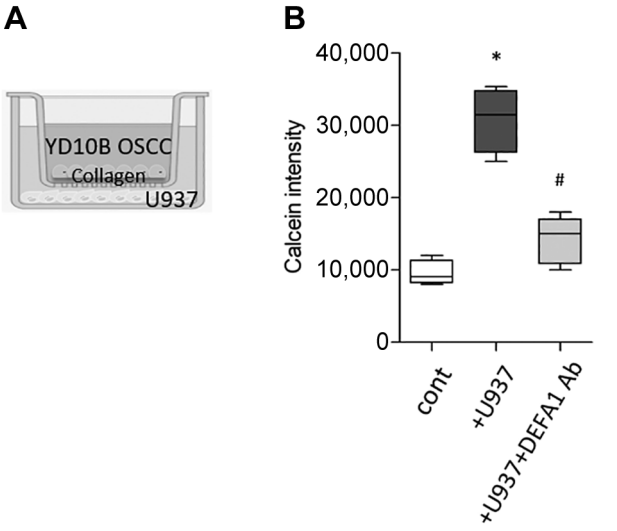

Figure 5. *Continued*

Discussion

Metastasis is a process in which cancer cells migrate from the primary tumor, requiring invasive cancer cells to traverse the basement membrane (BM). The BM serves as a natural barrier between the epithelium and the stroma, the latter being an extracellular matrix (ECM) network that houses various cell types (29). Cancer research has focused on genetic and epigenetic mutations within tumor cells. However, it is now proposed that the tumor micro-environment can significantly influence the biological characteristics of cancer. Consequently, research direction is shifting towards understanding interactions between cancer cells and stromal cells to control tumor progression, metastasis, recurrence, and drug resistance. Cancer invasion is often attributed to epithelial-mesenchymal transition (EMT), a mechanism where single cells dissociate and migrate independently. However, in actual cancer patient tissues, it is difficult to observe cells that are undergoing EMT, with most cases exhibiting collective invasion of invasive solid tumors (1). In collective invasion, cell-cell contact is maintained through cadherin, forming groups of aggregated cells that can invade collectively *via* ECM adhesion. Factors driving the individual *versus* collective migration of cancer cells are not fully understood yet. Nonetheless, amoeboid cells such as A375 and B16F2 melanoma cells tend to migrate individually or in streams, whereas epithelial cells migrate collectively. Cells with mesenchymal morphologies, such as MTLn3 or HT-1080, can switch between single-cell and collective migration

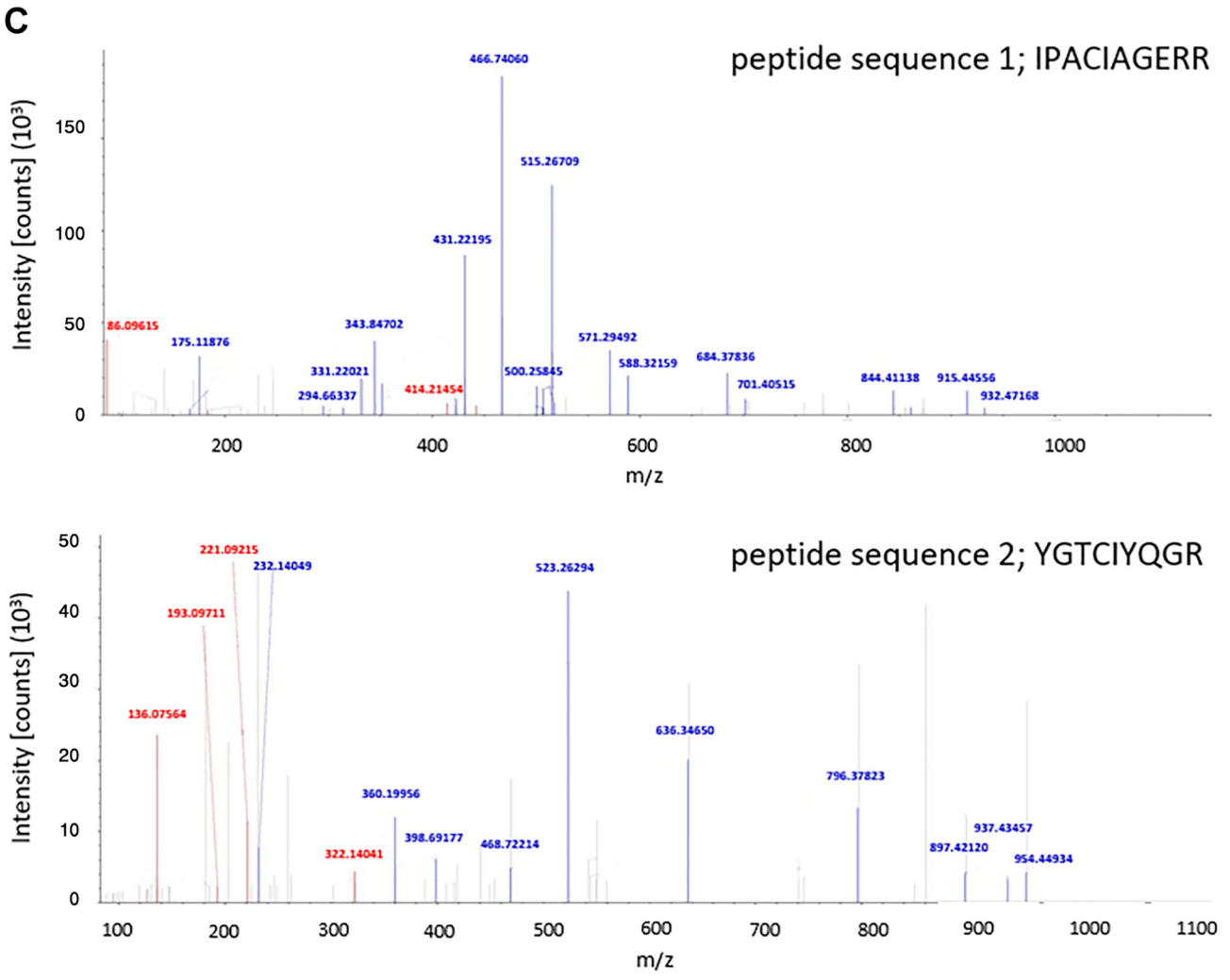

D

```
DEFA1      MRTLAILAAILLVALQAQAEPLQARADEVAAAPEQIAADIPEVVVSLAWDESLAWDESLAWDESLA
Peptide 1  ------------------------------------------------------------------
Peptide 2  ------------------------------------------------------------------

DEFA1      PKHPGSRKNMACYCRIPACIAGERRYGTCIYQGRLWFCC
Peptide 1  ---------------IPACIAGERR-----------
                          **********
Peptide 2  ------------------------YGTCIYQGR-----
                                   **********
```

Figure 5. *Continued*

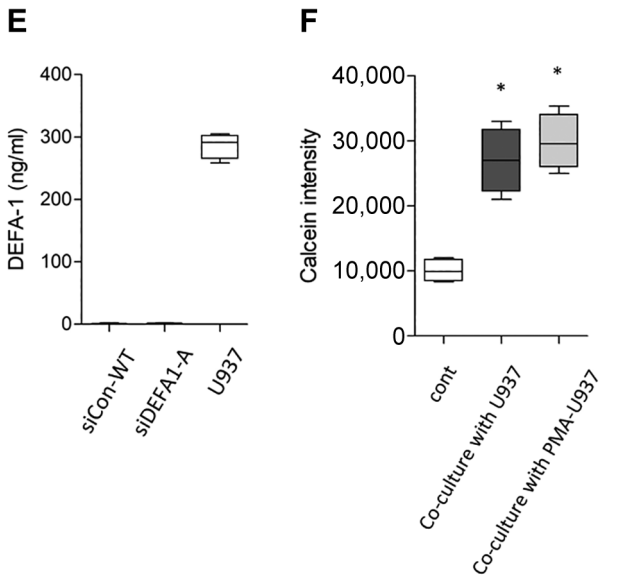

Figure 5. *Influence of U937 monocytic cells on cancer cell invasion. (A) Image showing the Transwell insert well and cell positioning used in co-culture experiments. (B) Impact of U937 cells on cancer cell invasion activity was observed through co-culture using a Transwell chamber. Calcein-AM-labeled siCon-WT cells were added to the Transwell insert well and U937 cells were added to the lower chamber in serum-free media for co-culture. After 24 h, cells in the lower chamber were harvested and fluorescence was analyzed. To observe DEFA1 antibody response in cancer cell invasion, a DEFA1 antibody (2 μg/ml) was added to both the Transwell insert well and the lower chamber for co-culture. *p<0.001 vs. siCon-WT, #p<0.01 vs. +U937. (C) DEFA1 peptide spectrum detected in conditioned media of U937 cells by LC-MS/MS analysis. Amino acid sequence peptide spectrum: peptide 1 - IPACIAGERR (up), peptide 2 - YGTCIYQGR (down). Peaks marked in red and blue indicate peaks matching each peptide sequence. (D) Alignment of the two peptide sequences detected in the LC-MS/MS analysis with the NCBI Reference Sequence of neutrophil defensin 1 (DEFA1) (Homo sapiens, NP_004075.11). (E) Quantification of DEFA1 by ELISA. DEFA1 levels in the conditioned media of YD10B siCon-WT, siDEFA1-A, and U937 cells was quantified. (F) Comparison of cancer cell invasion in a collagen-coated Transwell chamber between U937 cells treated with 100 nM phorbol 12-myristate 13-acetate (PMA-U937) and untreated U937 cells (U937) co-cultured with Calcein-AM-labeled cancer cells. *p<0.001 vs. siCon-WT (cont).*

modes. In hepatocyte growth factor (HGF)-treated MDCK cells, increased N-cadherin activity can promote the transition from individual invasion to collective cell migration. Collective invasion has been observed for various cancer types (6, 11, 30, 31). Group migration is characterized by sustained inter-cell adhesion and high directional movement with neighboring cells during migration. In collective invasive tissues, the invasive tumor front migrates as narrow linear strands led by leading cells or as broad, irregularly shaped sheets led by multiple leading cells. Leader cells at the invasive front guide the invasion, while follower cells at the tumor center follow their signals (1, 32). The fibrosis at the borderline between the tumor microenvironment (TME) and cancer cells has been reported to be associated with higher T classification, N classification, stage, histological grade, and invasion mode (33). In this study, we harvested the invasive tumor front area composed of leader cells and the tumor center area composed of follower cells from oral squamous cell carcinoma tissue exhibiting collective cancer invasion and compared their gene expression profiles. We confirmed that defensin 1-alpha (DEFA1) was highly expressed in cancer tissues compared to that in normal tissues. We also found that DEFA1 was especially expressed at a higher level in the invasive tumor front than in the tumor center of collective cancer invasion. Mass spectrometry separation and amino acid sequencing have revealed that alpha-defensins (human neutrophil peptides 1, 2, and 3) are expressed in squamous cell carcinoma tissue of human tongues (34). However, our study is the first to confirm high expression of DEFA1 at the invasive tumor front of collective cancer invasion. Considering accumulated reports that biological characteristics of cancer can be regulated by the tumor microenvironment, including cancer-associated fibroblasts (CAFs), tumor-associated macrophages (TAMs), and other immune and inflammatory cells (35), the high expression of DEFA1 at the invasive tumor front of collective cancer invasion adjacent to the cancer-surrounding stroma suggests that DEFA1 expression is likely to be regulated by the tumor microenvironment. Accordingly, we investigated not only the role of DEFA1 in cancer cells but also the regulation of DEFA1 expression by stromal cells around the tumor. High expression levels of DEFA1 at the invasive front of collective invasion were identified through microarray analysis of surgical tissues from three patients. To validate the findings obtained from small sample size, we used tissue immunostaining to reconfirm the overexpression of DEFA1 at the invasive front of collective invasion. Further

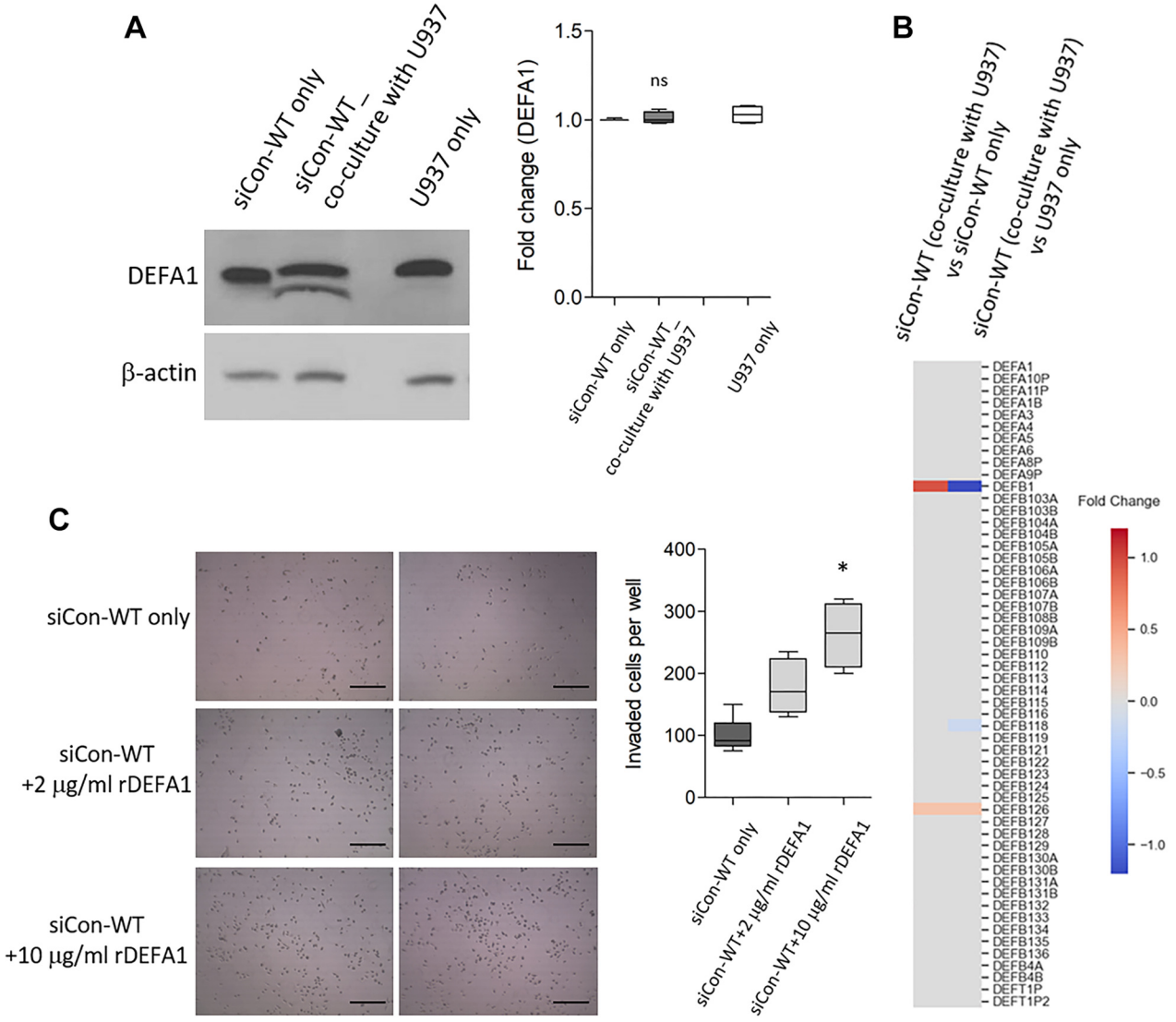

Figure 6. *DEFA1 expression and invasion of cancer cells co-cultured with U937 cells. (A) Analysis of DEFA1 expression in cancer cells (siCon-WT) co-cultured with U937 for 24 h using Western blot. β-Actin was used as a protein loading control. Intensity of the DEFA1 band is presented as a fold change. ns: Non-specific. (B) Hierarchical clustering heatmap. Expression changes of defensin isotypes due to co-culture were visualized using ExDEGA GraphicPlus. (C) Cancer cells (siCon-WT) were co-cultured with recombinant DEFA1 (rDEFA1; 2 μg/ml, 10 μg/ml) in Transwell inserts and incubated in 1% media. After 24 h, all cells attached to the lower chamber were counted. More than five repeated experiments were conducted. A representative result is provided (magnification; 100×, scale bars: 200 μm). Data are expressed as the mean±SD of three independent experiments. *p<0.001 vs. siCon-WT only.*

confirmation in a larger sample size is necessary to generalize our findings. Additionally, follow-up studies are needed to elucidate the intracellular signaling pathways and transcription factors involved in the overexpression of DEFA1.

Human defensins acting as antimicrobial peptides in the innate immune system are known to contribute to host defense by serving as a barrier in the epithelial layer against local infections (36). While defensins are known for their roles in cell division, immune cell attraction and maturation,

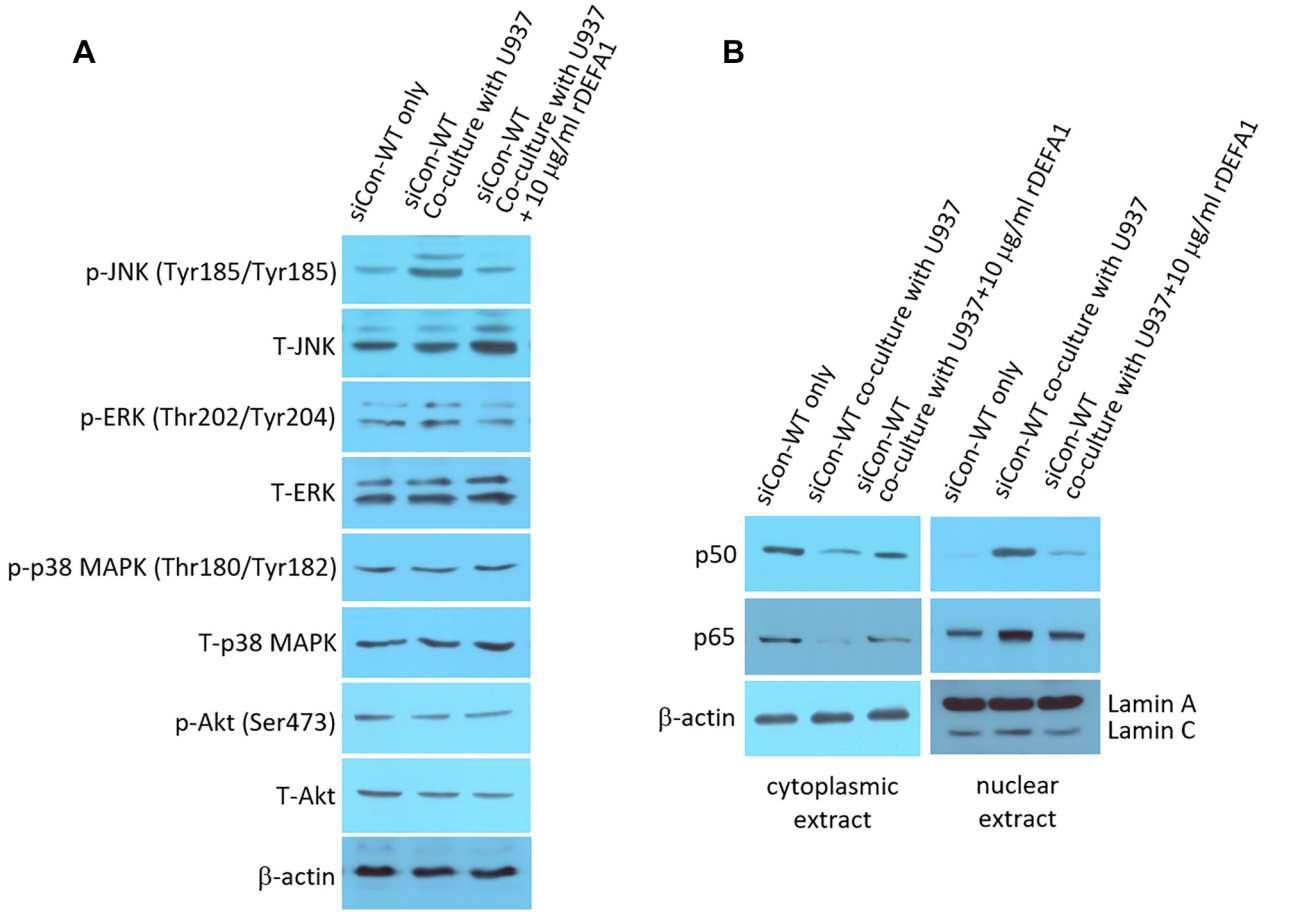

Figure 7. *Analysis of signal transduction molecules in cancer cells co-cultured with U937 monocytic cells. (A) Western blot analysis was conducted to assess the activation levels of mitogen-activated protein kinases (MAPKs) in siCon-WT cells co-cultured with U937. Activation was evaluated based on the phosphorylation levels of JNK, ERK1/2, p38 MAPK, and Akt. siCon-WT cells that were not co-cultured with U937 served as the control. Recombinant DEFA1 (rDEFA1, 10 μg/ml) was added into the co-culture media of U937 and siCon-WT. (B) Analysis of nuclear translocation of the transcription factor NF-κB in siCon-WT cells co-cultured with U937. The levels of NF-κB components p50 and p65 were analyzed in cytosolic and nuclear extracts obtained from the cells. β-actin and lamin A/C were used as loading controls for cytosolic and nuclear extracts.*

epithelial tissue differentiation and remodeling, wound healing, and tumor suppression, information on their roles in cancer invasion is still limited (37). Vertebrate defensins include α-DEFA and β-DEFA. Among six human α-DEFA isotypes, HNP1, HNP2, and HNP3 are encoded by *DEFA1* and *DEFA3* genes. They can be distinguished by a conserved cysteine motif, unlike *DEFA5* (HD5) and *DEFA6* (HD6) (38). Beta-defensin (HBD) acts as a tumor suppressor in some tumor types, while alpha-defensin (DEFA) promotes tumor cell growth or causes cell death at high concentrations (38, 39). Overexpression of DEFA1 has been observed in bladder cancer, colorectal cancer, and renal cell carcinoma (40-42), promoting tumor cell proliferation (42, 43) and contributing to tumor progression and invasiveness (40, 44). Our microarray analysis of gene expression profiling in the tumor center and invasive tumor front regions of collective cancer invasion revealed no significant difference in *HBD*, whereas *DEFA1* and *DEFA3* showed more than a 3-fold difference, with *DEFA1* being statistically significant. In our study, we constructed an oral cancer cell line with

suppressed *DEFA1* expression and confirmed that DEFA1 was involved in invasive activity and cancer growth through *in vitro* and *in vivo* studies. Cell lines inhibited DEFA1 expression showed reduced invasion without showing changes in cell cycle distribution, indicating the role of DEFA1 in cancer invasion. Tongue cancer established at an orthotopic site exhibited a significant reduction in tumor volume due to DEFA1 expression inhibition with foci-sized cell growth in multiple tissues. These results provide evidence for the role of DEFA1 in cancer progression at the invasive tumor front. We investigated the role of DEFA1 in cancer growth using a mouse xenograft model. While there are limitations in accurately replicating the human cancer growth environment, tumor xenograft models using immunocompromised mice are commonly employed as they most closely mimic the human cancer growth and metastasis environment. It has been reported that bladder cancer patients with increased tumor grade, lymphovascular invasion, and lymph node metastasis have higher plasma DEFA1-3 levels, suggesting that it could be used as a preliminary indicator for diagnosing cancer progression in bladder cancer patients (44). Additionally, plasma DEFA1-3 concentrations are elevated in patients with colon cancer (41, 45, 46). Although we attempted to detect DEFA1 in sera samples of xenografted mice, no significant concentration changes were measured. Further studies on the serum of oral cancer patients are needed to evaluate the potential of DEFA1 as a diagnostic marker for OSCC. This could contribute to the development of a tool for the more rapid diagnosis of OSCC.

Considering that a favorable environment for tumor growth and progression is created by tumor-associated fibroblasts (CAFs), tumor-associated macrophages (TAMs), and various immune and inflammatory cells within the tumor microenvironment, many studies have proposed strategies to simultaneously target cancer cells and the tumor microenvironment (47). In this study, we confirmed that cancer cell invasion was significantly increased through co-culture with U937 monocytic cells. Consistent with this, several studies have reported that monocyte-derived factors can regulate cancer activity. For example, prostate cancer cells co-cultured with U937 cells showed increased cancer invasion activity, which was inhibited by tissue factor neutralizing antibodies (48). Additionally, interleukin-6 (IL-6) secreted by monocytes could increase cancer cell migration and invasion by regulating EMT and promoting macrophage recruitment through C-C Motif Chemokine Ligand 2 (CCL2) (49). Monocytes co-cultured with MKN1 gastric cancer cells could differentiate into a tumor microenvironment (TME) producing matrix metalloproteinase-9 (MMP9), which could promote cancer invasion through ECM degradation (50). MMP-9 secreted by cancer cells not only can promote tumor progression and exacerbation by facilitating cancer cell migration and invasion by degrading the extracellular matrix (ECM), but also can regulates the migration and invasion of endothelial cells, thereby contributing to tumor-associated angiogenesis (51). In particular, CAFs can secrete IL-6 and granulocyte-macrophage colony-stimulating factor (GM-CSF) to differentiate monocytes into M2-like TAMs, thereby promoting tumor progression (52). Interestingly, we confirmed that increased cancer cell invasion by co-culture with U937 monocytic cells was significantly suppressed by a DEFA1 antibody. As a result of LC-MS/MS and ELISA analysis, DEFA1 (286.5±20.14 ng/ml) was detected in the culture medium of U937 cells. However, it was not detected at a significant concentration in the culture medium of cancer cells. These two results suggest that DEFA1 secreted from U937 cells can stimulate cancer invasion activity. In an invasion assay conducted at 24 h after treatment with recombinant DEFA1 (10 μg/ml) instead of co-culture with U937 cells, a significant increase in cancer cell invasion was found. These results imply that not only endogenous DEFA1, but also exogenous DEFA1 can regulate cancer invasion. Consistent with our results, the enhancement of cancer cell characteristics has been confirmed by exogenous DEFA (40). Exogenously treated DEFA can increase intracellular calcium ions influx, resulting in increased cell proliferation, motility, and invasiveness of bladder cancer cell lines. For this reason, they have proposed a role for autocrine tumor expression of DEFA in promoting the invasive phenotype of cancer cells. In our western blot analysis and gene expression profiling,

there was no further increase in DEFA1 expression in cancer cells co-cultured with U937 cells. Our results also indicated no autocrine action of DEFA1 in oral cancer cells and that exogenous DEFA1 might enhance cancer invasive activity through a mechanism separate from DEFA1 in cancer cells. Therefore, DEFA1 has a high potential to be developed as an inhibitor or a targeted immunotherapy agent, warranting further studies to explore its preclinical effects. In addition to the role of DEFA1 in enhancing tumor characteristics (40, 42-44), there have been reports on the regulation of cancer cell proliferation by exogenous DEFA1. As a result of the cell proliferation test observed for 48 h, a low concentration of DEFA1 (8 μg/ml) promoted epithelial cell proliferation of the KB squamous cell carcinoma cell line, while a high concentration of DEFA1 (50 μg/ml) was cytotoxic (43). In the renal cell carcinoma cell line A498, a mixture of α-defensins (DEFA-1, -2, and -3) at 12.5 μg/ml stimulated cell proliferation, whereas a mixture of α-defensins at a high concentration of >12.5 μg/ml caused cytotoxicity, such as inhibition of DNA synthesis (42).

In conclusion, our study not only demonstrated that DEFA1 plays an important role in cancer invasion, but also indicates that invasion can be enhanced by exogenous DEFA1 derived from the tumor microenvironment. We speculate that exogenous DEFA1 can regulate cancer invasion through a separate pathway rather than by further increasing DEFA1 expression in cancer cells. To clarify this, further studies are needed to determine the mechanism of interaction between cancer cells and monocytes. In addition, our study confirms that the invasive tumor front of collective cancer invasion is an area where cancer activity is closely regulated by the surrounding tumor microenvironment. Although further research is needed to fully understand implications of collective cancer invasion, it is clear that the invasive tumor front area is a highly strategic area for identifying targets that can diagnose and predict invasive cancer.

Conflicts of Interest

The Authors declare no competing interests.

Authors' Contributions

Conceptualization, S.P. and Y.H.; investigation, H.J., S.P. and Y.H.; writing, original draft preparation, H.J., S.P. and Y.H.; writing, review and editing, H.J., S.P. and Y.H.; project administration, H.J., S.P. and Y.H.; project administration, H.J., S.P. and Y.H. All Authors have read and agreed to the published version of the manuscript.

Funding

This research was supported by Eulji University in 2025 and the Basic Science Research Program through the National Research Foundation of Korea (NRF) funded by the Ministry of Education, Science and Technology (2022R1F1A1063204).

References

1 Friedl P, Locker J, Sahai E, Segall JE: Classifying collective cancer cell invasion. Nat Cell Biol 14(8): 777-783, 2012. DOI: 10.1038/ncb2548

2 Scarpa E, Mayor R: Collective cell migration in development. J Cell Biol 212(2): 143-155, 2016. DOI: 10.1083/jcb.201508047

3 Weaver AM: Invadopodia: Specialized cell structures for cancer invasion. Clin Exp Metastasis 23(2): 97-105, 2006. DOI: 10.1007/s10585-006-9014-1

4 Yang Y, Zheng H, Zhan Y, Fan S: An emerging tumor invasion mechanism about the collective cell migration. Am J Transl Res 11(9): 5301-12, 2019.

5 Yamamoto A, Doak AE, Cheung KJ: Orchestration of collective migration and metastasis by tumor cell clusters. Annu Rev Pathol 18(1): 231-256, 2023. DOI: 10.1146/annurev-pathmechdis-031521-023557

6 Miyazaki K, Togo S, Okamoto R, Idiris A, Kumagai H, Miyagi Y: Collective cancer cell invasion in contact with fibroblasts through integrin-α5β1/fibronectin interaction in collagen matrix. Cancer Sci 111(12): 4381-4392, 2020. DOI: 10.1111/cas.14664

7 Teeuwssen M, Fodde R: Cell heterogeneity and phenotypic plasticity in metastasis formation: the case of colon cancer. Cancers (Basel) 11(9): 1368, 2019. DOI: 10.3390/cancers 11091368

8 Ardila DC, Aggarwal V, Singh M, Chattopadhyay A, Chaparala S, Sant S: Identifying molecular signatures of distinct modes of collective migration in response to the microenvironment using three-dimensional breast cancer models. Cancers (Basel) 13(6): 1429, 2021. DOI: 10.3390/cancers13061429

9 Nakashima Y, Yoshinaga K, Kitao H, Ando K, Kimura Y, Saeki H, Oki E, Morita M, Kakeji Y, Hirahashi M, Oda Y, Maehara Y: Podoplanin is expressed at the invasive front of esophageal squamous cell carcinomas and is involved in collective cell invasion. Cancer Sci 104(12): 1718-1725, 2013. DOI: 10.1111/cas.12286
10 Hwang YS, Xianglan Z, Park KK, Chung WY: Functional invadopodia formation through stabilization of the PDPN transcript by IMP-3 and cancer-stromal crosstalk for PDPN expression. Carcinogenesis 33(11): 2135-2146, 2012. DOI: 10.1093/carcin/bgs258
11 Cheung KJ, Gabrielson E, Werb Z, Ewald AJ: Collective invasion in breast cancer requires a conserved basal epithelial program. Cell 155(7): 1639-1651, 2013. DOI: 10.1016/j.cell.2013.11.029
12 Yamaguchi N, Mizutani T, Kawabata K, Haga H: Leader cells regulate collective cell migration *via* Rac activation in the downstream signaling of integrin β1 and PI3K. Sci Rep 5: 7656, 2015. DOI: 10.1038/srep07656
13 Chrisafis G, Wang T, Moissoglu K, Gasparski AN, Ng Y, Weigert R, Lockett SJ, Mili S: Collective cancer cell invasion requires RNA accumulation at the invasive front. Proc Natl Acad Sci USA 117(44): 27423-27434, 2020. DOI: 10.1073/pnas.2010872117
14 Pflug KM, Lee DW, McFadden K, Herrera L, Sitcheran R: Transcriptional induction of NF-κB-inducing kinase by E2F4/5 facilitates collective invasion of GBM cells. Sci Rep 13(1): 13093, 2023. DOI: 10.1038/s41598-023-38996-9
15 Summerbell ER, Mouw JK, Bell JSK, Knippler CM, Pedro B, Arnst JL, Khatib TO, Commander R, Barwick BG, Konen J, Dwivedi B, Seby S, Kowalski J, Vertino PM, Marcus AI: Epigenetically heterogeneous tumor cells direct collective invasion through filopodia-driven fibronectin micropatterning. Sci Adv 6(30): eaaz6197, 2020. DOI: 10.1126/sciadv.aaz6197
16 Arima Y, Matsueda S, Saya H: Significance of cancer-associated fibroblasts in the interactions of cancer cells with the tumor microenvironment of heterogeneous tumor tissue. Cancers (Basel) 15(9): 2536, 2023. DOI: 10.3390/cancers15092536
17 Anderson NM, Simon MC: The tumor microenvironment. Curr Biol 30(16): R921-R925, 2020. DOI: 10.1016/j.cub.2020.06.081
18 Augoff K, Hryniewicz-Jankowska A, Tabola R: Invadopodia: clearing the way for cancer cell invasion. Ann Transl Med 8(14): 902, 2020. DOI: 10.21037/atm.2020.02.157
19 Toussaint LG 3rd, Nilson AE, Goble JM, Ballman KV, James CD, Lefranc F, Kiss R, Uhm JH: Galectin-1, a gene preferentially expressed at the tumor margin, promotes glioblastoma cell invasion. Mol Cancer 11: 32, 2012. DOI: 10.1186/1476-4598-11-32
20 Sanegre S, Eritja N, de Andrea C, Diaz-Martin J, Diaz-Lagares Á, Jácome MA, Salguero-Aranda C, García Ros D, Davidson B, Lopez R, Melero I, Navarro S, Ramon Y Cajal S, de Alava E, Matias-Guiu X, Noguera R: Characterizing the invasive tumor front of aggressive uterine adenocarcinoma and leiomyosarcoma. Front Cell Dev Biol 9: 670185, 2021. DOI: 10.3389/fcell.2021.670185
21 Lee MK, Zhang X, Kim HJ, Hwang YS: Peroxiredoxin 5 is involved in cancer cell invasion and tumor growth of oral squamous cell carcinoma. Oral Dis 29(2): 423-435, 2023. DOI: 10.1111/odi.13910
22 Pavlič A, Urh K, Boštjančič E, Zidar N: Analyzing the invasive front of colorectal cancer – By punching tissue block or laser capture microdissection? Pathol Res Pract 248: 154727, 2023. DOI: 10.1016/j.prp.2023.154727
23 Jeong D, Kim H, Kim D, Ban S, Oh S, Ji S, Kang D, Lee H, Ahn TS, Kim HJ, Bae SB, Lee MS, Kim CJ, Kwon HY, Baek MJ: Defensin alpha 6 (DEFA6) is a prognostic marker in colorectal cancer. Cancer Biomark 24(4): 485-495, 2019. DOI: 10.3233/CBM-182221
24 Lehrer RI, Lu W: α-Defensins in human innate immunity. Immunol Rev 245(1): 84-112, 2012. DOI: 10.1111/j.1600-065X.2011.01082.x
25 Dobin A, Davis CA, Schlesinger F, Drenkow J, Zaleski C, Jha S, Batut P, Chaisson M, Gingeras TR: STAR: ultrafast universal RNA-seq aligner. Bioinformatics 29(1): 15-21, 2013. DOI: 10.1093/bioinformatics/bts635
26 Anders S, Pyl PT, Huber W: HTSeq – a Python framework to work with high-throughput sequencing data. Bioinformatics 31(2): 166-169, 2015. DOI: 10.1093/bioinformatics/btu638
27 Kim JS, Cho IH, Kim KH, Hwang YS: Identification of galectin-10 as a biomarker for periodontitis based on proteomic analysis of gingival crevicular fluid. Mol Med Rep 23(2): 123, 2020. DOI: 10.3892/mmr.2020.11762
28 Hwang YS, Jeong M, Park JS, Kim MH, Lee DB, Shin BA, Mukaida N, Ellis LM, Kim HR, Ahn BW, Jung YD: Interleukin-1β stimulates IL-8 expression through MAP kinase and ROS signaling in human gastric carcinoma cells. Oncogene 23(39): 6603-6611, 2004. DOI: 10.1038/sj.onc.1207867
29 Winkler J, Abisoye-Ogunniyan A, Metcalf KJ, Werb Z: Concepts of extracellular matrix remodelling in tumour progression and metastasis. Nat Commun 11(1): 5120, 2020. DOI: 10.1038/s41467-020-18794-x
30 Gaggioli C, Hooper S, Hidalgo-Carcedo C, Grosse R, Marshall JF, Harrington K, Sahai E: Fibroblast-led collective invasion of carcinoma cells with differing roles for RhoGTPases in leading and following cells. Nat Cell Biol 9(12): 1392-1400, 2007. DOI: 10.1038/ncb1658
31 Nagai T, Ishikawa T, Minami Y, Nishita M: Tactics of cancer invasion: solitary and collective invasion. J Biochem 167(4): 347-355, 2020. DOI: 10.1093/jb/mvaa003
32 Wu JS, Jiang J, Chen BJ, Wang K, Tang YL, Liang XH: Plasticity of cancer cell invasion: Patterns and mechanisms. Transl Oncol 14(1): 100899, 2021. DOI: 10.1016/j.tranon.2020.100899
33 Tsuchihashi K, Nakatsugawa M, Kobayashi JI, Sasaya T, Morita R, Kubo T, Kanaseki T, Tsukahara T, Asanuma H, Hasegawa T, Hirano H, Miyazaki A, Hirohashi Y, Torigoe T: Borderline

microenvironment fibrosis is a novel poor prognostic marker of oral squamous cell carcinoma. Anticancer Res 40(8): 4319-4326, 2020. DOI: 10.21873/anticanres.14434

34 Lundy FT, Orr DF, Gallagher JR, Maxwell P, Shaw C, Napier SS, Gerald Cowan C, Lamey PJ, Marley JJ: Identification and overexpression of human neutrophil α-defensins (human neutrophil peptides 1, 2 and 3) in squamous cell carcinomas of the human tongue. Oral Oncol 40(2): 139-144, 2004. DOI: 10.1016/s1368-8375(03)00142-8

35 Mao X, Xu J, Wang W, Liang C, Hua J, Liu J, Zhang B, Meng Q, Yu X, Shi S: Crosstalk between cancer-associated fibroblasts and immune cells in the tumor microenvironment: new findings and future perspectives. Mol Cancer 20(1): 131, 2021. DOI: 10.1186/s12943-021-01428-1

36 Winter J, Wenghoefer M: Human defensins: potential tools for clinical applications. Polymers 4(1): 691-709, 2012. DOI: 10.3390/polym4010691

37 Adyns L, Proost P, Struyf S: Role of defensins in tumor biology. Int J Mol Sci 24(6): 5268, 2023. DOI: 10.3390/ijms24065268

38 Droin N, Hendra JB, Ducoroy P, Solary E: Human defensins as cancer biomarkers and antitumour molecules. J Proteomics 72(6): 918-927, 2009. DOI: 10.1016/j.jprot.2009.01.002

39 Xu D, Lu W: Defensins: a double-edged sword in host immunity. Front Immunol 11: 764, 2020. DOI: 10.3389/fimmu.2020.00764

40 Holterman DA, Diaz JI, Blackmore PF, Davis JW, Schellhammer PF, Corica A, Semmes OJ, Vlahou A: Overexpression of α-defensin is associated with bladder cancer invasiveness. Urol Oncol 24(2): 97-108, 2006. DOI: 10.1016/j.urolonc.2005.07.010

41 Melle C, Ernst G, Schimmel B, Bleul A, Thieme H, Kaufmann R, Mothes H, Settmacher U, Claussen U, Halbhuber KJ, Von Eggeling F: Discovery and identification of alpha-defensins as low abundant, tumor-derived serum markers in colorectal cancer. Gastroenterology 129(1): 66-73, 2005. DOI: 10.1053/j.gastro.2005.05.014

42 Müller CA, Markovic-Lipkovski J, Klatt T, Gamper J, Schwarz G, Beck H, Deeg M, Kalbacher H, Widmann S, Wessels JT, Becker V, Müller GA, Flad T: Human alpha-defensins HNPs-1, -2, and -3 in renal cell carcinoma: influences on tumor cell proliferation. Am J Pathol 160(4): 1311-1324, 2002. DOI: 10.1016/s0002-9440(10)62558-8

43 Nishimura M, Abiko Y, Kurashige Y, Takeshima M, Yamazaki M, Kusano K, Saitoh M, Nakashima K, Inoue T, Kaku T: Effect of defensin peptides on eukaryotic cells: primary epithelial cells, fibroblasts and squamous cell carcinoma cell lines. J Dermatol Sci 36(2): 87-95, 2004. DOI: 10.1016/j.jdermsci.2004.07.001

44 Gunes M, Gecit I, Pirincci N, Kemik AS, Purisa S, Ceylan K, Aslan M: Plasma human neutrophil proteins-1, -2, and -3 levels in patients with bladder cancer. J Cancer Res Clin Oncol 139(2): 195-199, 2013. DOI: 10.1007/s00432-012-1305-0

45 Melle C, Ernst G, Schimmel B, Bleul A, Thieme H, Kaufmann R, Mothes H, Settmacher U, Claussen U, Halbhuber K, Von Eggeling F: Discovery and identification of α-defensins as low abundant, tumor-derived serum markers in colorectal cancer. Gastroenterology 129(1): 66-73, 2005. DOI: 10.1053/j.gastro.2005.05.014

46 Albrethsen J, Bøgebo R, Gammeltoft S, Olsen J, Winther B, Raskov H: Upregulated expression of human neutrophil peptides 1, 2 and 3 (HNP 1-3) in colon cancer serum and tumours: a biomarker study. BMC Cancer 5: 8, 2005. DOI: 10.1186/1471-2407-5-8

47 Mayer S, Milo T, Isaacson A, Halperin C, Miyara S, Stein Y, Lior C, Pevsner-Fischer M, Tzahor E, Mayo A, Alon U, Scherz-Shouval R: The tumor microenvironment shows a hierarchy of cell-cell interactions dominated by fibroblasts. Nat Commun 14(1): 5810, 2023. DOI: 10.1038/s41467-023-41518-w

48 Lindholm PF, Lu Y, Adley BP, Vladislav T, Jovanovic B, Sivapurapu N, Yang XJ, Kajdacsy-Balla A: Role of monocyte-lineage cells in prostate cancer cell invasion and tissue factor expression. Prostate 70(15): 1672-1682, 2010. DOI: 10.1002/pros.21202

49 Chen X, Yang M, Yin J, Li P, Zeng S, Zheng G, He Z, Liu H, Wang Q, Zhang F, Chen D: Tumor-associated macrophages promote epithelial-mesenchymal transition and the cancer stem cell properties in triple-negative breast cancer through CCL2/AKT/β-catenin signaling. Cell Commun Signal 20(1): 92, 2022. DOI: 10.1186/s12964-022-00888-2

50 Kamoshida G, Matsuda A, Sekine W, Mizuno H, Oku T, Itoh S, Irimura T, Tsuji T: Monocyte differentiation induced by co-culture with tumor cells involves RGD-dependent cell adhesion to extracellular matrix. Cancer Lett 315(2): 145-152, 2012. DOI: 10.1016/j.canlet.2011.09.029

51 Zamanian M, Hajizadeh M, Shamsizadeh A, Moemenzadeh M, Amirteimouri M, Elshiekh M, Allahtavakoli M: Effects of naringin on physical fatigue and serum MMP-9 concentration in female rats. Pharm Biol 55(1): 423-427, 2017. DOI: 10.1080/13880209.2016.1244553

52 Cho H, Seo Y, Loke KM, Kim SW, Oh SM, Kim JH, Soh J, Lee H, Min JJ, Jung DW, Williams DR: Cancer-stimulated CAFs enhance monocyte differentiation and protumoral TAM activation *via* IL6 and GM-CSF secretion. Clin Cancer Res 24(21): 5407-5421, 2018. DOI: 10.1158/1078-0432.CCR-18-0125